Biochimica et Biophysica Acta 902 (1987) 349–359
Elsevier

BBA 73657

A Fourier-transform infrared spectroscopic study of the polymorphic phase behavior of 1,2-bis(tricosa-10,12-diynoyl)-*sn*-glycero-3-phosphocholine; a polymerizable lipid which forms novel microstructures

Alan S. Rudolph [a] and Thomas G Burke [b]

[a] *Biomolecular Engineering Branch, Naval Research Laboratory, Washington, DC and* [b] *Geo-Centers Inc, Suitland, MD (U S A)*

(Received 20 March 1987)

Key words 1,2-Bis(tricosa-10,12-diynoyl)-*sn*-glycero-3-phosphocholine, Diacetylenic phospholipid, Phase behavior, Phospholipid microstructure, Fourier-transform infrared spectroscopy

We have investigated the phase characteristics of 1,2-bis(tricosa-10,12-diynoyl)-*sn*-glycero-3-phosphocholine ($DC_{23}PC$), a phosphatidylcholine with diacetylenic groups in the acyl chains, and its saturated analog 1,2-ditricosanoyl-*sn*-glycero-3-phosphocholine (DTPC), using Fourier-transform infrared spectroscopy (FTIR). Previous studies on the phase behavior of $DC_{23}PC$ in H_2O have shown that $DC_{23}PC$ exhibits: (1) formation of cylindrical structures ('tubules') by cooling fluid phase multilamellar vesicles (MLVs) through T_m (43°C), and 2) metastability of small unilamellar vesicles (SUVs) in the liquid-crystalline state some 40°C below T_m, with subsequent formation of a gel phase comprised of multilamellar sheets at 2°C. The sheets form tubules when heated and cooled through T_m. FTIR results presented here indicate that as metastable SUVs are cooled toward the transition to bilayer sheets, spectroscopic changes occur before the calorimetric transition as measured by a reduction in the CH_2 symmetric stretch frequency and bandwidth. In spite of the vastly different morphologies, the sheet gel phase formed from SUVs is spectroscopically similar to the tubule gel phase. The C-H stretch region of $DC_{23}PC$ gel phase shows bands at 2937 and 2810 cm^{-1} not observed in the saturated analog of $DC_{23}PC$, which may be related to perturbations in the acyl chains introduced by the diacetylenic moiety. The narrow CH_2 scissoring mode at 1470 cm^{-1} and the prominent CH_2 wagging progression indicate that $DC_{23}PC$ gel phase was highly ordered acyl chains with extended regions of all-*trans* methylene segments. In addition, the 13 cm^{-1} reduction in the C = O stretch frequency (1733–1720 cm^{-1}) during the induction of $DC_{23}PC$ gel phase indicates that the interfacial region is dehydrated and rigid in the gel phase.

Abbreviations MLV, multilamellar vesicle, SUV, small unilamellar vesicles, $DC_{23}PC$, 1,2-bis(tricosa-10,12-diynoyl)-*sn*-glycero-3-phosphocholine, DTPC, 1,2-ditricosanoyl-*sn*-glycero-3-phosphocholine, DPPC, 1,2-dipalmitoyl-3-*sn*-phosphatidylcholine, $T_{m(C)}$, temperature of an exothermic event observed during a cooling scan, $T_{m(H)}$, temperature of an endothermic event observed during a heating scan, DSC, differential scanning calorimetry, FTIR, Fourier-transform infrared spectroscopy

Correspondence A S Rudolph, Biomolecular Engineering, Code 6190, Naval Research Laboratory, Washington, DC 20375 (U S A)

Induction

Phospholipid assemblies exist in a variety of morphologies in aqueous solution Of recent interest has been the aqueous filled cylindrical structures (or 'tubules', see Ref 1) formed in solution by the diacetylenic phospholipid 1,2-bis(tricosa-10,12-diynoyl)-*sn*-glycero-3-phosphocholine ($DC_{23}PC$) [1–4] The polymorphic phase behavior of this phospholipid and the molecular characteristics of the novel microstructures which it forms

have not been fully elucidated Such studies will aid in the development of these polymerizable assemblies for biotechnological applications as well as add to the understanding of phospholipid phase behavior The purpose of the present study is to use FTIR to investigate the structural features of the various polymorphic forms exhibited by the hydrated monomeric phospholipid and spectroscopically trace the thermal evolution of tubule formation from small unilamellar vesicles (SUVs) and multilamellar vesicles (MLVs) of $DC_{23}PC$

The formation of tubules from $DC_{23}PC$ has been observed by cooling fluid phase large MLVs through a phase transition at 43°C [1,2] The tubules consist of an aqueous core surrounded by multiple (2–10) bilayers, with diameters of 0 3–1 μm and lengths of up to hundreds of micrometers depending on conditions of formation [1–3] One of the mechanisms suggested by which tubules may form is the rolling or wrapping of vesicles of $DC_{23}PC$ [4]

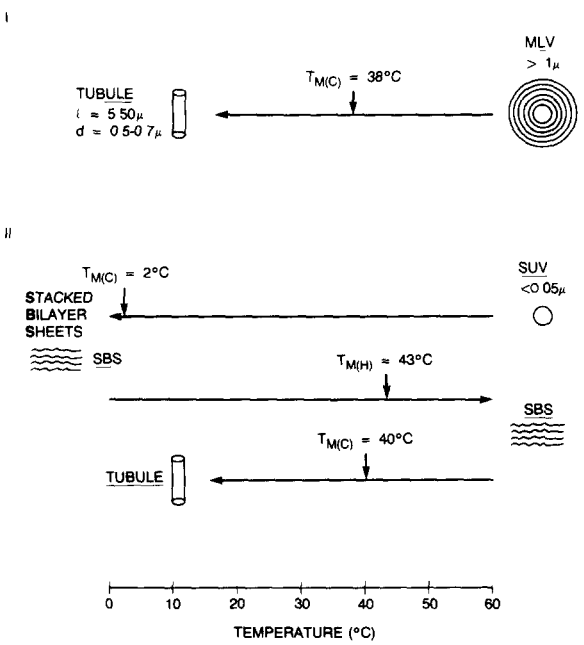

Fig 1 Polymorphic phase behavior of $DC_{23}PC$ Unagitated MLVs form tubules directly whereas SUVs are metastable and form a non-tubular low temperature phase comprised of stacked bilayer sheets (SBS) at 2°C which must then be heated above $T_{m(H)}$ and cooled through $T_{m(C)}$ before tubules will form This behavior is observed in both H_2O and ^2H_2O

A comparative study of the phase behavior of $DC_{23}PC$ and its saturated analog using DSC and freeze-fracture electron microscopy has demonstrated that the phase behavior of $DC_{23}PC$ may be dictated by the presence of the diacetylenic moiety and the initial morphology of the fluid phase [1] The same phase behavior was observed in ^2H_2O in the present work and is summarized in Fig 1 SUVs (0 04 + 0 01 μm) are metastable in the liquid-crystalline phase and, unlike large MLVs (outer diameter over 1 μm), do not form tubules directly upon cooling through the liquid-crystalline to gel phase transition (observed at 42°C) Instead, SUVs convert at 2°C to a non-tubular low-temperature phase which appears in freeze-fracture electron microscopic analysis to be extended regions of stacked lamellae (bilayer sheets) The stacked bilayer sheets form tubules when heated through the gel to liquid-crystalline phase transition and cooled back below T_m The formation of the novel gel phase morphologies from $DC_{23}PC$ liposomes may in part occur because of a requirement for reduced bilayer curvature in the gel phase [1] The phase behavior outlined was observed in both H_2O and ^2H_2O with only very minor changes in the values for transition temperatures and enthalpies Similar variations between H_2O and ^2H_2O are observed in the phase behavior of other phosphatidylcholines [6]

Infrared measurements have been successfully used to discern the molecular characteristics of phospholipid phase states (see Refs 7 and 8 for recent reviews) The changes induced in the spectra of phospholipids as they undergo phase transitions are quite marked, and can provide information about chain packing, lattice characteristics, head group hydration, and changes in the interfacial region of the bilayer [7–14] Preliminary infrared spectroscopic studies of $DC_{23}PC$ have shown that the dry, polycrystalline material at room temperature is highly ordered and spectroscopically resembles the subphase of saturated phosphatidylcholines [2,3] Previous Raman data on the monomeric hydrated tubule morphology has shown that the chains may be decoupled by the presence of the diacetylenic group [2,3] In addition, the low-frequency Raman spectra of the hydrated monomeric tubule structure reveals longitudinal acoustic modes which indicate that

the acyl chains are highly ordered (unpublished data)

In the present study we have correlated phase transitions in $DC_{23}PC$ suspensions observed by differential scanning calorimetry with spectroscopic changes determined by FTIR In addition, we have examined the saturated analog of DC_{23}-PC, 1,2-ditricosanoyl-*sn*-glycero-3-phosphocholine (DTPC), to compare pertinent spectral features and gain a better understanding of the structural differences between diacetylenic and saturated chain phosphatidylcholines

Materials and Methods

The lipid $DC_{23}PC$ was obtained as a gift from Dr A Singh The purity of the lipid was analyzed by thin-layer chromatography and yielded a single spot on silica gel 60 F-254 (E Merck) using a chloroform/methanol/water (65 25 4, v/v) solvent system with sample loadings of approx 1 mg lipid in 30 μl of solvent The saturated analog of $DC_{23}PC$, DTPC, was obtained from Avanti Polar Lipids (Birmingham, AL, U S A) and used without further purification All lipids used in these experiments were dried down from chloroform stock solutions and stored overnight in a vacuum desiccator to remove trace solvent Aliquots were then rehydrated with H_2O or ^2H_2O to a concentration of 100 mg/ml ^2H_2O was obtained from MSD isotopes (Montreal, Canada) H_2O used in these experiments was deionized and double glass distilled by a Corning MP-12A system (Corning, NY) SUVs were prepared by bath sonication (Laboratory Supply, Hicksville, NY) above $T_{m(H)}$ until optically clear The diameter of these vesicles is approximately 400 Å and has been characterized by freeze-fracture electron microscopy [1] Large MLVs were formed by hydration above $T_{m(H)}$ for 1 h without agitation This procedure has been shown in previous work to result in the formation of multilamellar vesicles with an average diameter of 0 5–3 μm [1–3] Samples were loaded into a calorimetry pan or the infrared sample cell at 50 °C, which is several degrees above $T_{m(H)}$ The data were collected after a 5–10 min equilibration period

Differential scanning calorimetric experiments were carried out on a Perkin-Elmer DSC-7 (Norwalk, CN) The calorimeter was calibrated for peak area and temperature using a sample of indium in a stainless steel pan Samples (40 μl) were loaded in stainless steel pans above $T_{m(H)}$ All of the samples were run against an equal weight of water at a scan rate of 1 °C/min The $T_{m(H)}$ and $T_{m(C)}$ values were determined from the peak temperature of the transitions Enthalpies were determined using lipid weights calculated from the weight fraction of the lipid in the suspension, and the total weight of suspension added to the pan The weight of lipid in each experiment was approximately 4 mg Under these conditions, $T_{m(H)}$ and ΔH values of 41 6 °C and 8 0 kcal/mol, respectively, were obtained for vortexed multilamellar vesicles of dipalmitoyl phosphatidylcholine, in agreement with previously reported values [15,16]

All of the spectra shown were recorded with a Perkin-Elmer 1750 FTIR spectrometer (Norwalk, CN) Data were collected over the infrared region 4000–400 cm^{-1} with 2 cm^{-1} resolution, at 1-cm^{-1} intervals and no zero filling BaF_2 windows with a 0 025 mm teflon spacer were loaded with 30 μl of a 100 mg/ml sample Temperature control was accomplished by placing the cell on an aluminium water jacket which mounts in the compartment cell of the instrument [17] This temperature-controlled jacket was connected to a programmable water bath and temperature controlled to 0 1 °C The temperature of the sample was monitored by attaching a thermocouple to one of the windows The rate of temperature change used in these experiments was 1 °C/min Spectral deconvolution was done interactively through an enhancement software subroutine supplied by Perkin Elmer The lorentzian line widths chosen for this procedure are described with the pertinent spectra and care was taken in manipulations of this sort [18,19]

Samples for freeze-fracture analysis were examined at the same concentration as the calorimetric and spectroscopic experiments Once the phase behavior was confirmed by calorimetry, the sample was removed from the pan and loaded onto copper specimen plates After freezing in melted nitrogen, the specimen plates were then transferred to a Balzers 400D (Hudson, NH) and

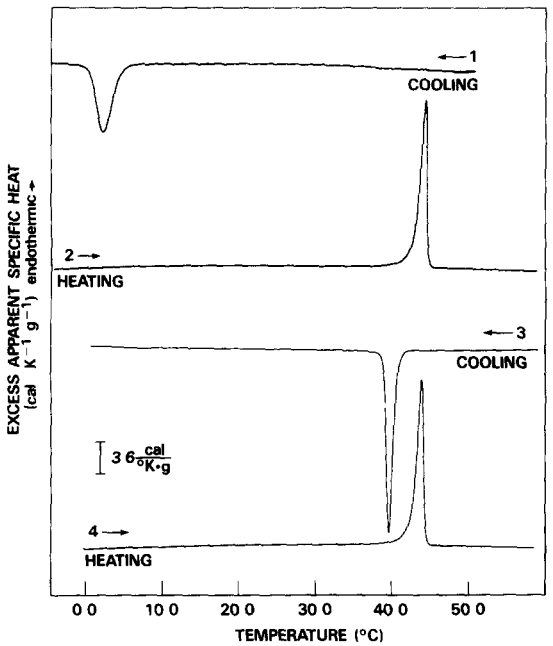

Fig 2 Calorimetric scans of $DC_{23}PC$ SUVs in ^2H_2O Scan 1 is the initial cooling curve which shows the metastability of these vesicles An exotherm at 2 4° C is observed which is the transition to the stacked bilayer sheet gel phase (see Fig 3a and b) The enthalpy of this transition is −22 kcal/mol Scan 2 is the heating thermogram of this phase, showing a $T_{m(H)}$ of 43 1° C and enthalpy of 23 kcal/mol, respectively Subsequent cooling of the sample resulted in an exotherm at 38 3° C ($T_{m(C)}$) with an enthalpy of −23 kcal/mol, which is correlated by freeze-fracture with the transition to the tubule gel phase Scan 4 is the heating scan of the tubule low-temperature phase with $T_{m(H)}$ at 43 3° C and enthalpy of 23 kcal/mol

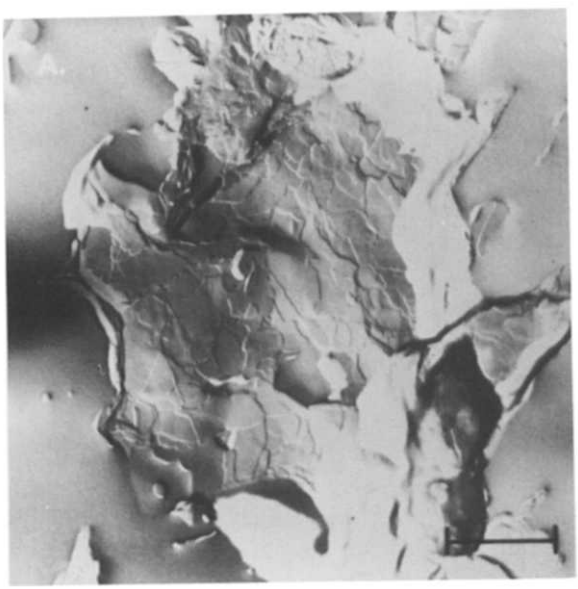

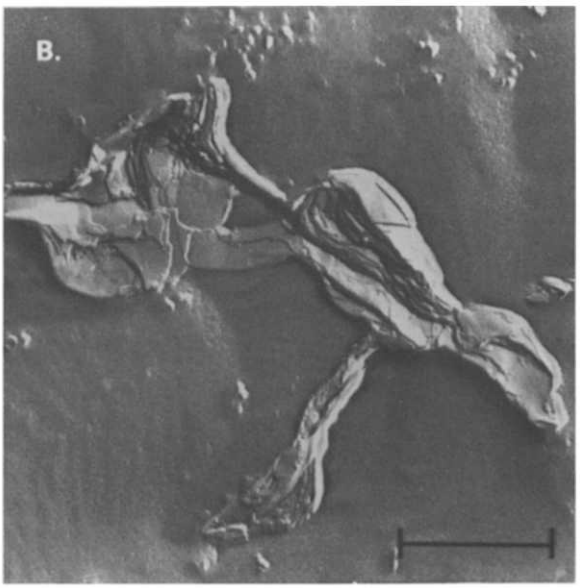

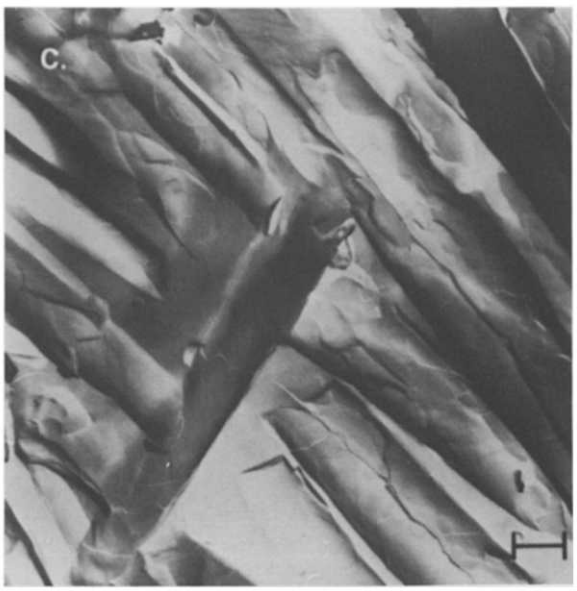

Fig 3 Freeze-fracture micrographs of the two different morphologies observed in the gel phase of $DC_{23}PC$ (A) Extended regions of bilayer sheets are generated by cooling SUVs below 2° C, (magnification, 32K) (B) The bilayer sheets formed during this transition are stacked, note two fracture planes in this figure, with cross-fracture showing multiple stacked layers of sheets, (magnification, 45K) (C) The tubule structures seen in this micrograph were formed from cooling bilayer sheets through $T_{m(C)}$ (magnification, 15K) These same structures form directly from MLVs by cooling through $T_{m(C)}$ All scale bars, 0 5 μm

fractured and replicated at −110 °C Replicas were washed with sodium hypochlorite and transferred to copper grids for electron microscopic examination which was accomplished with a Zeiss 10CA (Thornwood, NY)

Results and Discussion

The formation of the stacked sheet gel phase from metastable SUVs

Fig 2 shows a series of calorimetric scans of a 100 mg/ml suspension of SUVs of $DC_{23}PC$ in ^2H_2O Scan 1 shows that as the vesicles are cooled an exothermic phase transition is observed at 2 4 °C, with an enthalpy of −22 kcal/mol Figs 3A and B show freeze-fracture replicas of the structures formed from this transition The morphology of this phase consists of large regions of stacked multilamellar sheets (note stacks in cross-fracture plane, Fig 3B) No tubular or vesicular structures were observed

Although cooling SUVs showed no bulk phase transition observed by calorimetry until 2 4 °C, changes were observed in FTIR spectra The C-H stretch region for SUVs cooled toward the transition to stacked bilayer sheets is seen in Fig. 4A As the temperature is cooled, there is a shift in the CH_2 asymmetric and symmetric stretch frequencies At 50 °C, these bands are broad and observed at 2927 and 2854 cm^{-1}, respectively At 10 °C, the asymmetric stretch shifts to 2920 cm^{-1} and has a multicomponent appearance (middle spectra, Fig 4A) The frequency and full bandwidth at half peak height for the CH_2 symmetric stretch of the SUVs as they are cooled to form the stacked bilayer sheets are seen in Fig 5 As the vesicles are cooled toward this transition, the frequency decreases from 2854 at 50 °C to 2851 cm^{-1} at 20 °C (Fig 5A), with a 3 cm^{-1} reduction

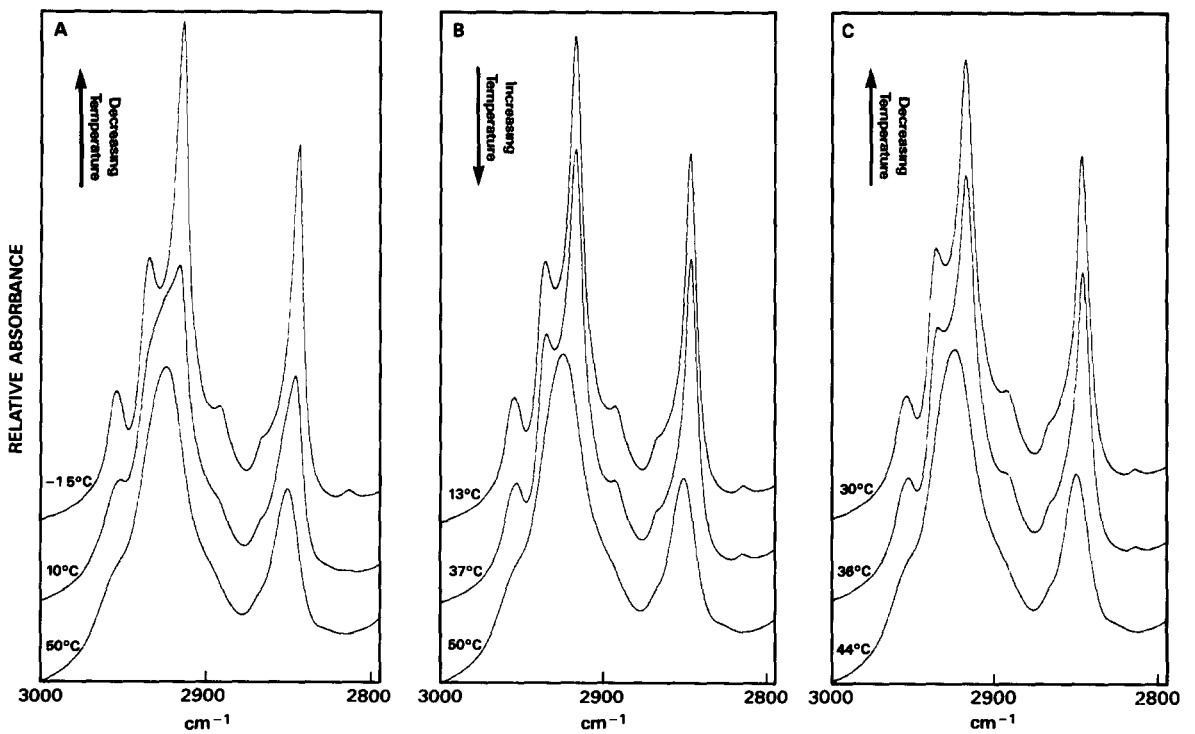

Fig 4 FTIR spectra of the C-H stretch region of $DC_{23}PC$ during the thermal formation of tubules from cycling SUVs in ^2H_2O Spectra have been offset to better aid comparison (A) Cooling of SUVs and the formation of stacked bilayer sheets, scans shown are 50, 10, −1 5 °C (B) Heating stacked bilayer sheets above $T_{m(H)}$, scans shown are 13, 37, 50 °C (C) The subsequent formation of tubules, scans shown at 44, 36, 30 °C

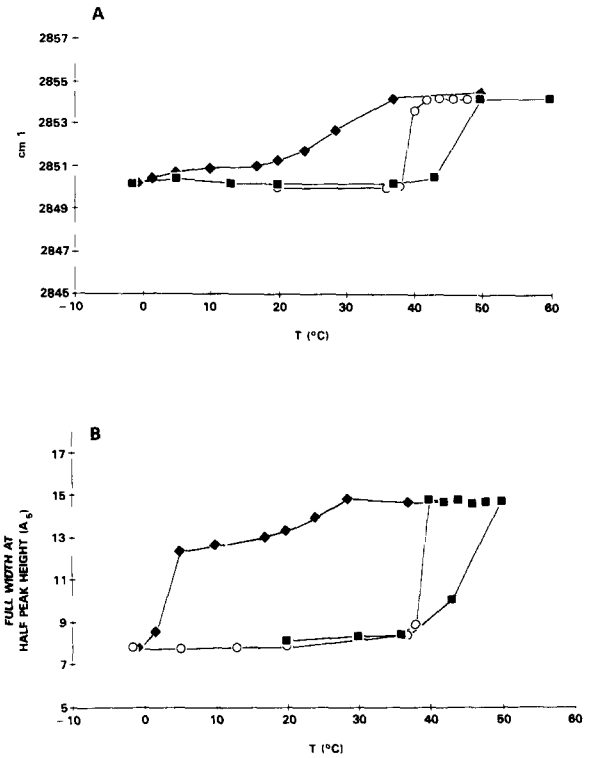

Fig 5 Frequency and full width at half peak height of the CH_2 symmetric stretch during the indirect thermal formation of tubules from SUVs in ^2H_2O (a) Frequency vs temperature plot for the indirect formation of tubules from SUVs ◆, Cooling SUVs, and the formation of stacked bilayer sheets, ■, heating stacked bilayer sheets above $T_{m(H)}$, ○, cooling stacked bilayer sheets and the formation of tubules (b) Full bandwidth at half peak height vs temperature plot during the indirect formation of tubules from SUVs ◆, Formation of stacked bilayer sheets from SUVs ■, heating the stacked bilayer sheets above $T_{m(H)}$, ○, tubule formation from cooling fluid sheets

in the bandwidth of the CH_2 symmetric stretch over this temperature range (Fig 5B)

The carbonyl stretch region observed in the spectra of the vesicles at 50 °C reveals a broad peak centered at 1733 cm^{-1} (Fig 6) Infrared spectra of aqueous dispersions of liquid-crystalline DPPC show a broad C = O stretch frequency centered at 1735 cm^{-1} [7–9] Deconvolution or derivative spectra of the C = O stretching band of DPPC reveal that it is comprised of two overlapping broad bands centered at approximately 1742 and 1725 cm^{-1}, which represent the *sn*-1 and *sn*-2 C = O frequencies, respectively [7–10,20] Changes in the C = O stretching bands are dependent on the thermal history of the sample, but usually

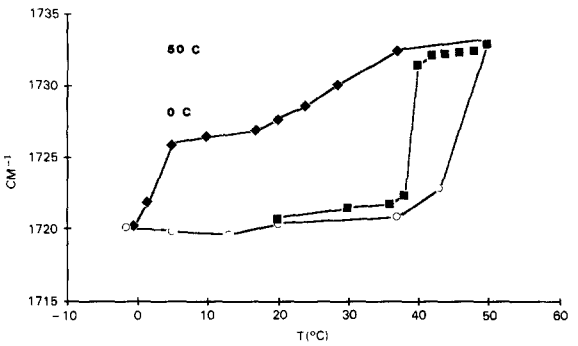

Fig 6 The change in the C = O stretch frequency during the thermal formation of tubules in ^2H_2O ◆, Cooling SUVs and the formation of the sheet gel phase ○, heating the stacked bilayer sheets above $T_{m(H)}$ ■, Cooling through $T_{m(C)}$ and the formation of the tubule gel phase Inset shows spectral deconvolution (lorentzian line width, 16 cm^{-1}) of the C = O stretch of liquid-crystalline $DC_{23}PC$ (top spectrum, peaks at 1739, 1733, 1726, 1718 cm^{-1}) and gel phase $DC_{23}PC$ (bottom spectrum, peaks at 1739, 1733, 1722, 1718 cm^{-1}), which reveals that the observed reduction in the C = O frequency is due to a shift in the relative intensities of the *sn*-1 and *sn*-2 bands

involve changes in the relative peak heights of the *sn*-1 and *sn*-2 vibration The deconvoluted spectrum of liquid-crystalline $DC_{23}PC$ at 50 °C (inset, Fig 6) shows that this band is comprised of four broad bands at 1739, 1733, 1726 and 1718 cm^{-1}, with the greatest intensity observed in the vibration at 1733 cm^{-1} These four bands may represent different rotational isomers of the C = O, and suggests that there is significantly more conformational order in this region than observed in liquid-crystalline C = O spectra of saturated phosphatidylcholines Cooling the SUVs to 10 °C results in a 6 cm^{-1} reduction in the frequency of the broad C = O stretch This decrease indicates that the packing and interfacial environment of the vesicles changes before the observed calorimetric phase transition These differences could reflect changes in the hydration of the head group region as the metastable SUVs are cooled toward the transition to bilayer sheets Experiments are currently underway to investigate the role of SUV fusion in the formation of bilayer sheets, and these vesicle-vesicle interactions may play a role in the observed FTIR changes in metastable SUVs

The transition to the sheet gel phase from SUVs was observed in spectra taken between 5 and −1 5 °C which correlates to the temperature range

in which the bulk phase transition to the sheet gel phase is observed by DSC The C = O stretch at −1 5 °C shows a sudden 6 cm^{-1} decrease in the frequency of this vibration (Fig 6) The deconvolution of this spectrum reveals that the relative peak height of the observed bands has changed with peaks observed at 1739, 1733, 1722 and 1717 cm^{-1}, with the greatest intensity in the peak at 1717 cm^{-1} (inset, Fig 6) The 13 cm^{-1} decrease in the C = O stretch of $DC_{23}PC$ as a result of the formation of the sheet gel phase (Fig 6) indicates that the dielectric environment of the C = O has changed and that this phase has an interfacial region with reduced hydration [8,9] The C = O frequency observed in the gel phase of $DC_{23}PC$ and the bandwidth (21 cm^{-1}) indicates that it is very similar to the subgel phase of DPPC in which the water of hydration in the head group is reduced [20]

In the C-H stretch region (Fig 4A, top spectra at −1 5 °C), the sheet gel phase shows a marked increase in the peak height of the CH_2 asymmetric and symmetric stretches, with the peaks found at 2919 and 2850 cm^{-1}, respectively There are also bands at 2937 and 2810 cm^{-1} which were not previously resolved in liquid-crystalline spectra Figs 5A and B show the change in the frequency and bandwidth of the CH_2 symmetric stretch during the formation of the sheet gel phase There is little change in the frequency of this band at the transition temperature, but a 5 cm^{-1} change in the full width at half peak height

The increase in peak height and reduced bandwidth of the CH_2 stretching vibrations and the reduction in frequency as a result of the formation of the sheet gel phase is indicative of the increase in the *trans/gauche* ratio in the acyl chains and reflects the increase in conformational order in this region Similar changes have been observed in the liquid-crystalline to gel phase transition of saturated phosphatidylcholines [7,8] Significant differences in the C-H stretch region of $DC_{23}PC$ and saturated chain phosphatidylcholines do exist, however The appearance of bands at 2937 and 2810 cm^{-1} in the gel phase spectra of $DC_{23}PC$ may indicate that different vibrational populations of methylene segments exist These may arise as a result of the diacetylenic moiety as these bands are not observed in the saturated analog, DTPC (see Fig 9B) Different vibrational populations could arise from methylene segments on separate sides of this moiety ($-CH_2-CH_2-CH_2-C\equiv C-C\equiv C-{}^*CH_2-{}^*CH_2-{}^*CH_2-$) Alternatively, this result could represent methylene segments

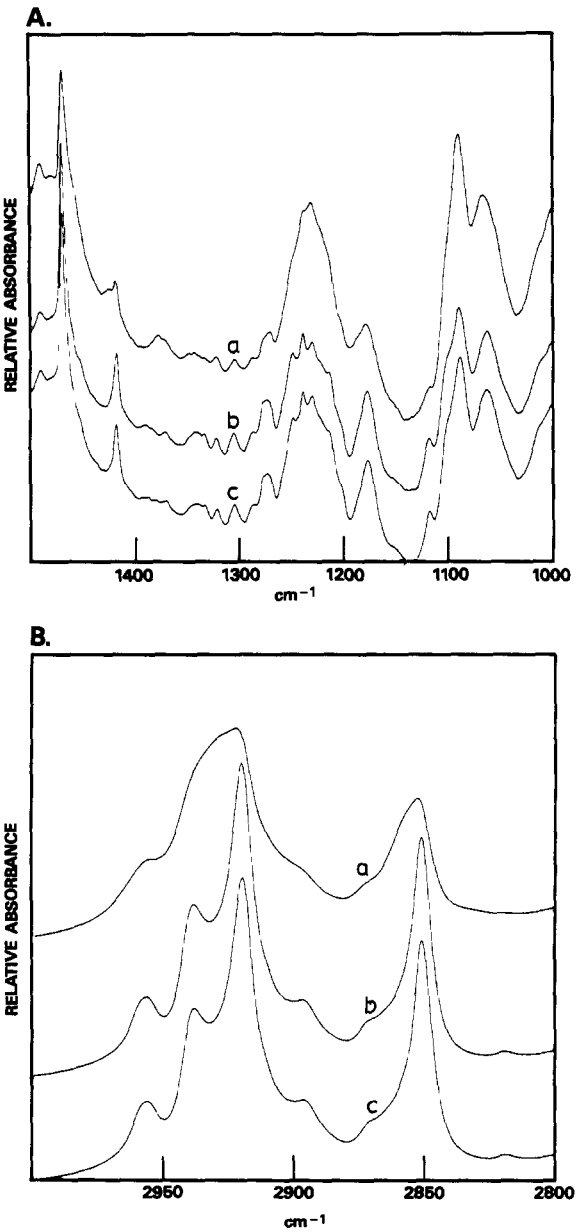

Fig 7 Comparison of different morphologies of $DC_{23}PC$ at 20 °C (A) fingerprint region, 1500–1000 cm^{-1} (a) SUVs, (b) stacked bilayer sheets, (c) tubules (B) C-H stretch region, 3000–2800 cm^{-1} (a) SUVs, (b) stacked bilayer sheets, (c) tubules

closest to the diacetylene on either side of this moiety (CH_2-*CH_{22}-*CH_2-C≡C-C≡C-*CH_2-*CH_2-CH_2-) Preliminary FTIR experiments on a series of $DC_{27}PC$ lipids with varying position of the diacetylenic group in the acyl chains has revealed that the perturbation introduced by this moiety is a local one, affecting methylenes on either side of the diacetylene (unpublished data)

Further indication that the bilayer sheets have highly ordered acyl chains is evident in the spectra seen in Fig 7A The prominent CH_2 wagging progression observed between 1350 and 1175 cm^{-1} (with peaks at 1333, 1322, 1305, 1277, 1249, 1238, 1229 and 1213 cm^{-1}) indicates that the acyl chains consist of many all-*trans* methylene segments [21,22]

Heating stacked bilayer sheets above T_m

Fig 2, scan 2 shows the calorimetric scan of the slow heating of the bilayer sheet gel phase The transition observed at 2.4°C upon cooling was not observed as the sample was heated through this range Further heating results in an endotherm at 43.8°C ($T_{m(H)}$) with an enthalpy of 23 kcal/mol The corresponding infrared spectra of the C-H stretch region in Fig 4B indicate that as this sample is heated there is a slight decrease in the peak height and broadening of the asymmetric and symmetric stretches Overall though, Figs 5A and B show that there is little change in the frequency and full bandwidth at half peak height of the CH_2 symmetric stretch during the slow heating of this phase (from 0 to 30°C) At 35°C, the band at 2937 cm^{-1} is broadened and it is not observed in spectra taken above $T_{m(H)}$ Above $T_{m(H)}$, the asymmetric and symmetric stretches are found at 2927 and 2854 cm^{-1} and the spectral features return to those observed in fluid-phase SUVs Freeze-fracture analysis has shown that the bilayer sheets morphology is retained above $T_{m(H)}$ [1] The relatively little change in the spectra as the stacked bilayer sheets are heated toward $T_{m(H)}$ indicates that this phase has tightly packed acyl chains which may be resistant to thermally induced conformational change

The formation of tubules from cooling stacked bilayer sheets

The calorimetric scan for the formation of tubules upon cooling the lipid through $T_{m(C)}$ is seen in Fig 2 (scan 3) As the sample is cooled, an exotherm is observed at 38°C which freeze-fracture analysis showed to correspond to tubule formation (see Fig 3C) Fig 4C shows the changes in the C-H stretch region during the formation of tubules from this fluid phase At 36°C, the C-H asymmetric stretch is at 2919 cm^{-1}, with the band at 2937 cm^{-1} observed as the tubule gel phase is formed. Figs. 5A and B show that at the transition temperature, the frequency decreases 4 cm^{-1} and the bandwidth approximately 7 cm^{-1} This figure also confirms the observed calorimetric result that this phase transition is hysteretic (compare $T_{m(C)}$ and $T_{m(H)}$ in Fig. 2, scans 2 and 3)

Examination of Fig. 7 shows that in spite of widely differing morphologies gel phase tubules and bilayer sheets have very similar spectroscopic characteristics The acyl chains in both exhibit a remarkable degree of crystallinity and are highly ordered, with bands at 2937 and 2810 cm^{-1} which may be ascribed to methylenes perturbed by the presence of the diacetylenic group The prominent wagging progression is observed in both gel-phase sheets and tubules Comparison of the full width at 3/4 peak height of the CH_2 methylene bending vibration (6 1 cm^{-1} for sheets and 6 3 cm^{-1} for tubules) indicates that the gel-phase tubules and sheets may have similar packing characteristics The deconvoluted C = O stretch spectra show similar frequencies and relative intensities, indicating similarities in the interfacial region (data not shown)

The formation of tubules from cooling large MLVs

The inset of Fig 8 shows two DSC thermograms of a $DC_{23}PC$ MLV suspension in ^2H_2O at 60°C Upon cooling (scan 1), an exothermic event is observed with $T_{m(C)}$ and H values of 38 3°C and −22 kcal/mol, respectively Upon heating the tubular gel phase, an endothermic event occurred at a $T_{m(H)}$ value of 43 8°C, with an enthalpy change of 23 kcal/mol

Under the same experimental conditions used in the calorimetry experiments, a $DC_{23}PC$ MLV suspension was cooled in the FTIR spectrometer and several spectra, shown in Fig 8, were recorded as the sample was cooled As the sample is cooled, there is an abrupt change in the spectra

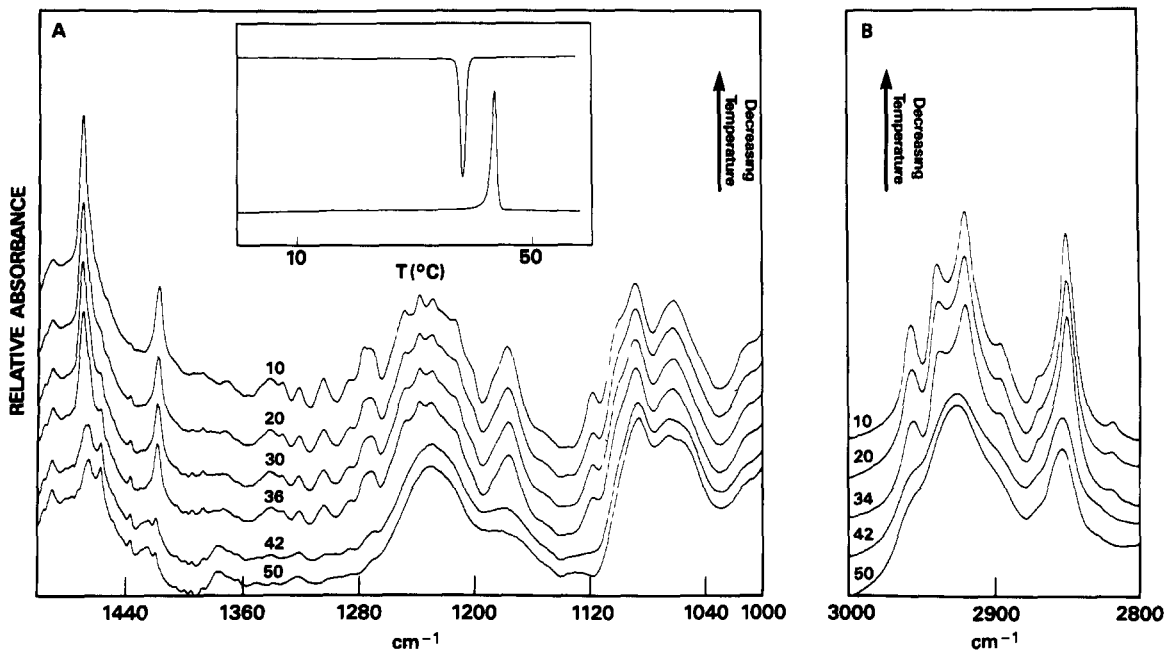

Fig 8 (A) Inset shows DSC cooling and heating thermograms of an MLV suspension of $DC_{23}PC$ in ^2H_2O Values for the transition temperatures and enthalpies can be found in text Below inset are FTIR spectra of identical samples at various temperature points during the cooling cycle Spectra have been offset to better aid comparisons Lower spectra is at 50 °C, with spectra above at 42, 36, 30, 20 and 10 °C (B) CH_2 stretch region Lower spectra is at 50 °C, with spectra above at 42, 34, 20 and 10 °C

observed between the spectra at 42 and 36 °C, the same temperature range at which the DSC reveals a bulk phase transition in the sample Fig 8a reveals that tubules formed from MLVs are spectroscopically similar in this region to those formed from sheets, the methylene scissoring mode sharpens and shifts to 1470 cm^{-1} (from 1465 cm^{-1}) and the methylene wagging progression is prominent between 1375 and 1177 cm^{-1} There is a marked increase in the CH_2 deformation at 1418 cm^{-1} [13] and the skeletal vibrations at 1177, 1118 and 1063 cm^{-1}, indicating that the acyl chains have become more rigid as conformational order is introduced in this phase

Overall, the spectral features of tubules formed from MLVs are similar to tubules formed from SUVs There are, however, some subtle differences The full width at 3/4 peak height of the CH_2 scissoring mode (1470 cm^{-1}) at 20 °C in tubules formed from MLVs is 8 3 cm^{-1}, while for SUVs it is 6 3 cm^{-1} In addition, the band ratio of the 2937 and 2919 cm^{-1} band is different in the tubules formed from MLVs (MLVs have a higher 2937 cm^{-1} component, see Fig 8B) The alteration in this ratio may be due an increased width of the 2920 cm^{-1} asymmetric CH_2 stretch These subtle changes in tubules formed from MLVs and indirectly from SUVs may also arise as the MLVs represent a vesicle population of heterogeneous size distribution from which tubules form The outer lamellae of the MLV may form tubules directly upon cooling while the inner lamellae (or smaller MLVs) may have a reduced curvature sufficient to exhibit metastability, and not form tubules directly Previous studies have shown that smaller vortexed multilamellar vesicles (average diameter, 0 3–0 4 μm) did exhibit metastability below $T_{m(H)}$ and did not form tubules directly (unpublished data) SUVs, on the other hand, represent a homogeneous population of vesicles which convert completely to stacked bilayer sheets and, upon cycling, efficiently convert to tubules These spectroscopic differences may not relate to efficiency of tubule formation and we cannot rule out the possibility that tubules formed from MLVs are inherently less ordered than those formed indirectly from SUVs

The saturated analog of $DC_{23}PC$

Aqueous suspensions of the saturated analog of $DC_{23}PC$, DTPC, were spectroscopically examined (in ^2H_2O), and the spectra are shown in Figs 9A and B This lipid does not form tubules [1–3] Fig 9A reveals that the CH_2 scissoring mode displays crystal field splitting in the gel phase of this lipid (at 20 °C), with two bands at 1472 and 1462 cm^{-1}, which is indicative of an orthorhombic lattice type [5,20,21] Previous calorimetric data has shown a main melting transition at 77 °C with another smaller transition at 28 °C, which may be a subgel transition [1] The C-H stretch region of this lipid reveals two broad peaks above T_m (data not shown) at 2923 and 2852 cm^{-1}, which represent the asymmetric and symmetric stretches, respectively At 20 °C these peaks are found at 2917 and 2849 cm^{-1} Fig 9B shows the C-H stretching region for DTPC liposomes in the gel phase at 20 °C, together with the C-H manifold for tubules recorded at the same temperature The symmetric (2850 cm^{-1}) and the asymmetric (2920 cm^{-1}) stretching modes of DTPC are significantly broader than those of $DC_{23}PC$ This reflects the significantly tighter packing and increased rigidity of the acyl chains in the gel phase of $DC_{23}PC$ relative to DTPC The significantly more ordered chain region of $DC_{23}PC$ indicates there are unusually tight packing requirements dictated by the presence of the diacetylenic group and that this may be an important factor in tubule formation

Conclusion

We have investigated the phase characteristics of the $DC_{23}PC$ by FTIR This lipid displays two vastly different morphologies in the gel phase which appear spectroscopically similar The C-H stretch spectra reflect the local perturbation introduced by the diacetylenic moiety, with the appearance of vibrationally distinct methylene populations The decreased frequency of the C = O stretch and the increase in the relative peak height of the *sn*-2 C = O stretch indicates that the gel phase of $DC_{23}PC$ has a head group region with significantly reduced hydration Tubules formed

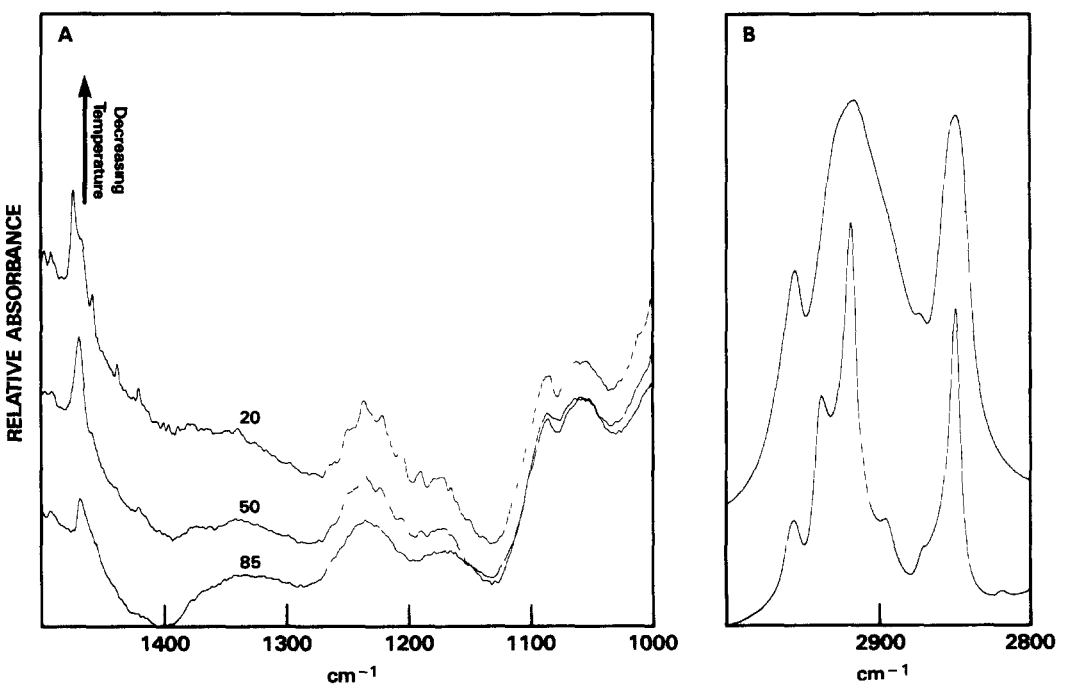

Fig 9 FTIR spectra of DTPC (A) Cooling DTPC vesicles, spectra from top at 20, 50 and 85 °C (B) Comparison of the C-H stretch region of DTPC with the $DC_{23}PC$ tubule gel phase formed from cycling SUVs Both spectra shown at 20 °C Spectra have been offset to aid comparison

from MLVs have the same general spectroscopic signature as those formed indirectly from SUVs, but appear slightly more disordered This disorder may be indicative of incomplete conversion of MLVs to tubules, with the presence of metastable vesicles below $T_{m(C)}$, or reflect subtle differences in tubule formation The gel phase of $DC_{23}PC$ is significantly more ordered than the saturated chain analog The amount of conformational order in the freshly formed tubules is comparable to that observed in the subgel phase of DPPC It is important to note that the subgel phase of DPPC is arrived at through time-dependent annealing at low temperature, whereas $DC_{23}PC$ tubules show this high degree of conformational order as this phase is formed The polymorphism displayed by gel phase $DC_{23}PC$ may provide information about the requirements for tubule formation It appears that the formation of gel-phase sheets from SUVs fulfills a requirement for a morphology of reduced curvature from which tubules will form We speculate that the formation of tubules from liquid-crystalline bilayer sheets may occur by wrapping or rolling of sheets as the lipid is cooled through T_m, as has been suggested for the formation of tubules from MLVs [4] The exact mechanism by which this occurs is still unknown Further experiments in our laboratory will be aimed at extending our studies of tubule formation and studying the spectroscopic changes induced upon the polymerization of this material

Acknowledgements

We would like to thank Ron Price, James P Sheridan and Barbara Herendeen for their technical support and helpful discussions and Alok Singh for the generous gift of $DC_{23}PC$

References

1 Burke, T G , Sheridan, J P , Singh, A and Schoen, P (1986) Biophys J 49, 321a
2 Yager, P and Schoen, P (1984) Mol Cryst Liq Cryst 106, 371–381
3 Schoen, P E and Yager, P (1985) J Polymer Sci 23, 2203–2216
4 Yager, P , Schoen, P E , Davies, C , Price, R and Singh, A (1985) Biophys J 48, 899–906
5 Yager, P , Schoen, P , Georger, J , Price, R and Singh, A (1986) Biophys J 49, 302a
6 Lipka, G , Chowdry, B Z and Sturtevant, J M (1984) J Phys Chem 88, 5401
7 Casal, H L and Mantsch, H H (1984) Biochim Biophys Acta 779, 381–401
8 Levin, I W (1984) in Advances in Infrared and Raman Spectroscopy, Vol 11 (Clark, R J H , and Hester, R E , eds), pp 1–48, Wiley Heyden, New York
9 Bush, S F , Adams, R G and Levin, I W (1980) Biochemistry 19, 4429–4435
10 Bush, S F , Levin, H and Levin, I W (1980) Chem Phys Lipids 27, 101–111
11 Cameron, D G , Gudgin, E F and Mantsch H H (1981) Biochemistry 20 4496–4500
12 Fookson, J E and Wallach, D F H (1978) Arch Biochem Biophys 189, 195–204
13 Mantsch, H H , Cameron, D G , Tremblay, P A and Kates, M (1982) Biochim Biophys Acta 689, 63–72
14 Parker, F S (1983) Applications of Infrared Spectroscopy in Biochemistry, Biology and Medicine, pp 142–165, Plenum Press, New York
15 Mabry, S and Sturtevant, J M (1978) Methods Membrane Biol 9, 237
16 Chowdhry, B Z and Dalziel, A W (1985) Biochemistry 24, 4109
17 Cameron, D G and Jones, R N (1981) Appl Spectrosc 35, 448
18 Kauppinen, J K , Moffatt, D J , Mantsch, H H and Cameron, D G (1981) Appl Spectrosc 35, 271–276
19 Kauppinen, J K , Moffatt, D J , Cameron, D G and Mantsch, H H (1981) Appl Optics 20, 1866–1879
20 Cameron, D G and Mantsch, H H (1982) Biophys J 38, 175–184
21 Snyder, R G (1979) J Chem Phys 71, 3229–3235
22 Snyder, R G and Schachtschneider, J H (1963) Spectrochim Acta 19, 85–116